J|A|C|S ARTICLES

Published on Web 08/17/2009

Measurement of Methyl Group Motional Parameters of Invisible, Excited Protein States by NMR Spectroscopy

D. Flemming Hansen, Pramodh Vallurupalli, and Lewis E. Kay*

Departments of Molecular Genetics, Biochemistry, and Chemistry, The University of Toronto, Toronto, Ontario, Canada M5S 1A8

Received May 13, 2009; E-mail: kay@pound.med.utoronto.ca

Abstract: An understanding of many biological processes can only be achieved through studies of the structure (enthalpy) and motions (entropy) of the key molecules that are involved, including those that are formed only transiently and with low population. These transiently formed, low populated states are invisible to most biophysical techniques but in many cases they can be studied in detail using relaxation dispersion NMR spectroscopy. Relaxation dispersion methodology has recently been described for the measurement of protein backbone excited state chemical shifts as well as bond vector orientations, which form the basis for structural studies of these invisible conformers. It is of interest to extend such studies by quantifying motional parameters of the excited state, providing a more complete description of the energy landscape that drives the biochemical event in question. Herein we describe a relaxation dispersion method for measuring site-specific motional parameters of methyl containing residues in the excited state. The approach is applied to the invisible unfolded state of the G48M Fyn SH3 domain that is in exchange with the folded conformation. Not surprisingly, the degree of disorder is in general higher in the unfolded state than in the folded conformer, although there is some ordering of side-chains in the unfolded state toward the C-terminal region of the domain. The development of the present methodology provides the first step toward characterizing the motional properties of invisible conformers, complementing the structural information that is already available from relaxation dispersion studies.

Introduction

It is becoming increasingly clear that biological molecules are dynamic over a broad spectrum of time-scales and that often these dynamics are related to function.[1−5] Insight into the relation between motion and function has been obtained from detailed experimental studies using standard tools of structural biology such as X-ray diffraction and NMR spectroscopy only in cases where the intermediates involved in a particular process can be stabilized. However, in cases where conformers are formed transiently and are of low population they are often invisible to many of the biophysical methods that are in routine use so that insight into their structure and dynamics is less forthcoming.[6] In principle, solution NMR spectroscopy is a powerful probe of functional biomolecular dynamics because molecular processes with time-scales ranging from ps (for example, bond vector librations) to hours (local or global unfolding) can affect NMR observables.[7] For example, molecular dynamics on the ms time-scale, frequently important in many biological processes such as ligand binding, protein folding and enzyme catalysis,[8−12] causes line broadening of NMR signals and can be studied by the Carr−Purcell−Meiboom−Gill (CPMG) spin relaxation dispersion experiment.[13−15] Here chemical exchange between a predominant state (referred to in what follows as the ground state) and one or more low populated (excited) states can be probed so long as the mole fraction of the latter exceeds ∼0.5%. Parameters describing the kinetics and thermodynamics of the exchange process are obtained from analysis of the resulting relaxation dispersion profiles. Most importantly, it is also possible to directly obtain chemical shifts

(1) Karplus, M.; Kuriyan, J. *Proc. Natl. Acad. Sci. U.S.A.* **2005**, *102*, 6679–6685.
(2) Henzler-Wildman, K. A.; Lei, M.; Thai, V.; Kerns, S. J.; Karplus, M.; Kern, D. *Nature* **2007**, *450*, 913–916.
(3) Lange, O. F.; Lakomek, N. A.; Fares, C.; Schroder, G. F.; Walter, K. F.; Becker, S.; Meiler, J.; Grubmuller, H.; Griesinger, C.; de Groot, B. L. *Science* **2008**, *320*, 1471–1475.
(4) Boehr, D. D.; McElheny, D.; Dyson, H. J.; Wright, P. E. *Science* **2006**, *313*, 1638–1642.
(5) Min, W.; English, B. P.; Luo, G.; Cherayil, B. J.; Kou, S. C.; Xie, X. S. *Acc. Chem. Res.* **2005**, *38*, 923–931.
(6) Hansen, D. F.; Vallurupalli, P.; Kay, L. E. *J. Biomol. NMR* **2008**, *41*, 113–120.
(7) Mittermaier, A.; Kay, L. E. *Science* **2006**, *312*, 224–228.
(8) Feher, V. A.; Baldwin, E. P.; Dahlquist, F. W. *Nat. Struct. Biol.* **1996**, *3*, 516–521.
(9) Sugase, K.; Dyson, H. J.; Wright, P. E. *Nature* **2007**, *447*, 1021–1024.
(10) Korzhnev, D. M.; Salvatella, X.; Vendruscolo, M.; Di Nardo, A. A.; Davidson, A. R.; Dobson, C. M.; Kay, L. E. *Nature* **2004**, *430*, 586–590.
(11) Wolf-Watz, M.; Thai, V.; Henzler-Wildman, K.; Hadjipavlou, G.; Eisenmesser, E. Z.; Kern, D. *Nat. Struct. Mol. Biol.* **2004**, *11*, 945–949.
(12) Vallurupalli, P.; Kay, L. E. *Proc. Natl. Acad. Sci. U.S.A.* **2006**, *103*, 11910–11915.
(13) Carr, H. Y.; Purcell, E. M. *Phys. Rev.* **1954**, *54*, 630–638.
(14) Meiboom, S.; Gill, D. *Rev. Sci. Instrum.* **1958**, *29*, 688–691.
(15) Palmer, A. G.; Kroenke, C. D.; Loria, J. P. *Methods Enzymol.* **2001**, *339*, 204–238.

of NMR active probes in the exchanging states[15,16] that are sensitive reporters of structure.[17,18] To date, experiments are available for measuring a wide range of excited state protein chemical shifts including those from ^{15}N, ^{1}HN, $^{13}C^{\alpha}$, $^{13}C^{\beta}$, ^{13}CO and $^{1}H^{\alpha}$ spins,[6,19−23] which form the basis for predicting backbone dihedral angles,[24] as well as side-chain $^{13}C_{methyl}$ shifts.[25] Recently, a new class of CPMG experiment has been developed which enables the determination of bond vector orientations in excited protein states that also provides valuable structural restraints.[26−28] The first structure of an invisible, excited conformer corresponding to the ligand-bound form of an SH3 domain based exclusively on data obtained from CPMG dispersion experiments recently appeared, establishing the utility of the methodology.[29]

In addition to quantifying the thermodynamic parameters of the exchange reaction[30] (ΔG, ΔH, $T\Delta S$) through a temperature dependent dispersion study and characterizing the structural features of excited states, it is also important to understand their site-specific dynamics, which can be related to residue-specific contributions to conformational entropy.[31−33] Experimental methods for probing site-specific motional properties of these transiently populated conformers have not been reported to date. Here too, the CPMG experiment is of utility since, in principle, it is sensitive to the intrinsic ps−ns time-scale motions of each of the exchanging conformers.[34] Analysis of dispersion data is most often carried out neglecting differences in the dynamics of the ground and excited states, simplifying the analysis considerably with little effect on the extracted exchange parameters in the majority of cases.[34,35] In situations where significant differences in ps-ns time-scale dynamics in the ground and excited states exist we show here that by using spin-state selective relaxation dispersion NMR spectroscopy it becomes possible to extract transverse relaxation rates of NMR probes in the exchanging conformers. Thus, motional parameters of the invisible, excited state are obtained, complementing the structural information that is also forthcoming from the analysis. In what follows we illustrate the methodology through a study of the ps-ns dynamics of methyl groups from Ile, Leu and Val residues in an "invisible", unfolded state of a G48M mutant Fyn SH3 domain which exchanges with the folded state on the ms time-scale.

Results and Discussion

Measuring Motional Parameters in Invisible States. Figure 1a illustrates an "exchange event" linking ground and excited protein states which is probed using the ^{13}C nucleus of a methyl group in the molecule. In addition to the conformational change there is also a change in the dynamics of the methyl group in each of the two states, with the amplitude of motion larger in the excited state in this example. Amplitudes of motion are most often characterized by an order parameter squared, S^2, that ranges from 0 (isotropic motion) to 1 (completely restricted motion).[36] If the exchange event is slow ($k_{ex} = k_{AB} + k_{BA} < \Delta\omega_{AB} = \omega_A - \omega_B$, ω is the chemical shift in rad/s) to intermediate ($k_{ex} \approx \Delta\omega_{AB}$) on the chemical shift time-scale, separate resonance lines are, in principle, observed for a probe in each of the exchanging states. In practice the line derived from the excited state (state "B") is most often not observed since its population is low and for k_{ex} on the ms time-scale the exchange contribution to the line-widths of B-state peaks ($\sim 1/k_{BA}$) is on the order of hundreds of Hz.[6,15]

The key to the measurement of methyl dynamics in the excited state is to isolate each of the four ^{13}C lines of the methyl quartet ($\mathbf{C}_+^{\alpha\alpha\alpha}$, $\mathbf{C}_+^{\alpha\alpha\beta}$, $\mathbf{C}_+^{\alpha\beta\beta}$, $\mathbf{C}_+^{\beta\beta\beta}$), where α and β denote the up and down spin states for each of the three proton spins of the methyl group, Figure 1*b*, and to perform separate experiments on each line. Thus, proton spin-state selective relaxation dispersion profiles are recorded, Figure 1*c*, that measure the transverse ^{13}C relaxation rate ($R_{2,eff}$) as a function of the number of chemical shift refocusing pulses (proportional to ν_{CPMG}). Dispersion profiles ($R_{2,eff}$ vs ν_{CPMG}) are sensitive reporters of $\Delta\omega_{AB}$; they are modulated by ν_{CPMG} because increasing the number of refocusing pulses decreases the effective chemical shift difference between states, $\Delta\omega_{eff}$. Thus, as ν_{CPMG} is increased the exchange process effectively moves toward the fast-exchange regime, $k_{ex}/\Delta\omega_{eff}$ increases, and in the limit of fast pulsing such that $\Delta\omega_{eff} \rightarrow 0$ the dispersion profiles become flat with $R_{2,eff}$ approaching the population weighted average of the intrinsic relaxation rates of probes in each state.[37] In the case where the intrinsic relaxation rates of the probes (in this example ^{13}C) in each of the two exchanging states are the same, the four dispersion profiles are expected to be offset with respect to each other, but otherwise equivalent (see below). By contrast, more substantial differences are anticipated for the case where the motional properties of each state are distinct. Consider, for example, the situation of slow chemical exchange so that the exchange contribution to transverse relaxation of each probe in the ground state A, $R^A_{2,eff}$, is given by k_{AB}; that is, $R^A_{2,eff}(\nu_{CPMG} = 0) = R^A_{2,int} + k_{AB}$, where $R^A_{2,int}$ is the intrinsic relaxation rate in the absence of exchange. In the fast pulsing limit the exchange process is "driven" into the fast regime (i.e., $k_{ex} \gg \Delta\omega_{eff}$) and $R^A_{2,eff}(\nu_{CPMG} \rightarrow \infty) = p_A R^A_{2,int} + p_B R^B_{2,int}$, where p_A and $p_B = 1 - p_A$ are the fractional populations of states A and B, respectively. Thus, the "size" of the dispersion profile (Figure 1*d*), $R_{2,ex} =$

(16) Skrynnikov, N. R.; Dahlquist, F. W.; Kay, L. E. *J. Am. Chem. Soc.* **2002**, *124*, 12352–12360.
(17) Cavalli, A.; Salvatella, X.; Dobson, C. M.; Vendruscolo, M. *Proc. Natl. Acad. Sci. U.S.A.* **2007**, *104*, 9615–9620.
(18) Shen, Y.; et al. *Proc. Natl. Acad. Sci. U.S.A.* **2008**, *105*, 4685–4690.
(19) Loria, J. P.; Rance, M.; Palmer, A. G. *J. Am. Chem. Soc.* **1999**, *121*, 2331–2332.
(20) Tollinger, M.; Skrynnikov, N. R.; Mulder, F. A. A.; Forman-Kay, J. D.; Kay, L. E. *J. Am. Chem. Soc.* **2001**, *123*, 11341–11352.
(21) Ishima, R.; Torchia, D. *J. Biomol. NMR* **2003**, *25*, 243–248.
(22) Ishima, R.; Baber, J.; Louis, J. M.; Torchia, D. A. *J. Biomol. NMR* **2004**, *29*, 187–198.
(23) Hansen, D. F.; Vallurupalli, P.; Lundstrom, P.; Neudecker, P.; Kay, L. E. *J. Am. Chem. Soc.* **2008**, 2667–2675.
(24) Cornilescu, G.; Delaglio, F.; Bax, A. *J. Biomol. NMR* **1999**, *13*, 289–302.
(25) Lundstrom, P.; Vallurupalli, P.; Religa, T. L.; Dahlquist, F. W.; Kay, L. E. *J. Biomol. NMR* **2007**, *38*, 79–88.
(26) Vallurupalli, P.; Hansen, D. F.; Stollar, E. J.; Meirovitch, E.; Kay, L. E. *Proc. Natl. Acad. Sci. U.S.A.* **2007**, *104*, 18473–18477.
(27) Igumenova, T. I.; Brath, U.; Akke, M.; Palmer, A. G. *J. Am. Chem. Soc.* **2007**, *129*, 13396–13397.
(28) Hansen, D. F.; Vallurupalli, P.; Kay, L. E. *J. Am. Chem. Soc.* **2008**, *130*, 8397–8405.
(29) Vallurupalli, P.; Hansen, D. F.; Kay, L. E. *Proc. Natl. Acad. Sci. U.S.A.* **2008**, *105*, 11766–11771.
(30) Korzhnev, D. M.; Kay, L. E. *Acc. Chem. Res.* **2008**, *41*, 442–451.
(31) Akke, M.; Bruschweiler, R.; Palmer, A. *J. Am. Chem. Soc.* **1993**, *115*, 9832–9833.
(32) Yang, D.; Kay, L. E. *J. Mol. Biol.* **1996**, *263*, 369–382.
(33) Li, Z.; Raychaudhuri, S.; Wand, A. J. *Protein Sci.* **1996**, *5*, 2647–2650.
(34) Ishima, R.; Torchia, D. A. *J. Biomol. NMR* **2006**, *34*, 209–219.
(35) Millet, O.; Loria, J. P.; Kroenke, C. D.; Pons, M.; Palmer, A. G. *J. Am. Chem. Soc.* **2000**, *122*, 2867–2877.
(36) Lipari, G.; Szabo, A. *J. Am. Chem. Soc.* **1982**, *104*, 4546–4559.
(37) Cavanagh, J.; Fairbrother, W. J.; Palmer, A. G.; Skelton, N. J. *Protein NMR Spectroscopy: Principles and Practice*; Academic Press: San Diego, 1996.

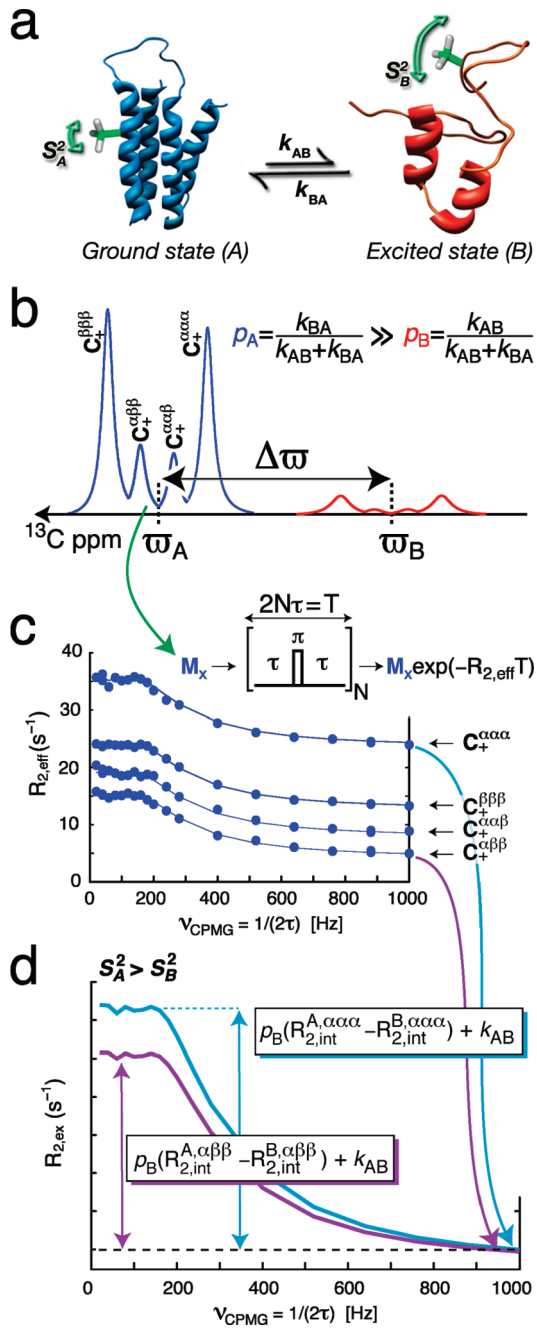

Figure 1. Measurement of methyl group dynamics in invisible, excited protein states. (a) Exchange between ground and excited protein states where the amplitude of ps−ns time-scale dynamics in the ground state is less than in the excited state, $S_A^2 > S_B^2$. (b) Carbon NMR spectrum of the exchanging methyl group of (a). The spectrum of the excited state is shown (red); normally it is not observed due to the short lifetime of the excited state ($1/k_{BA}$) and its low population (p_B). The scalar coupling between the methyl ^{13}C and its three directly attached protons splits the carbon spectrum into four lines (for example, $\mathbf{C}_+^{\alpha\alpha\beta}$ denotes the carbon transition where two of the three attached protons are in the $|\alpha\rangle$ spin-state). (c) Individual CPMG relaxation dispersion profiles are recorded for each the four lines and (d) the differences between the four relaxation dispersion profiles, $\mathbf{C}_+^{\alpha\alpha\alpha}$, ..., $\mathbf{C}_+^{\beta\beta\beta}$, are used to derive intrinsic transverse relaxation rates, $R^{B,\alpha\alpha\alpha}_{2,int}$, ...,$R^{B,\beta\beta\beta}_{2,int}$, of the excited state that can be interpreted in terms of ps−ns dynamics parameters.

$R_{2,\mathrm{eff}}(\nu_{\mathrm{CPMG}} = 0) - R_{2,\mathrm{eff}}(\nu_{\mathrm{CPMG}} \to \infty) = p_B(R^{\mathrm{A}}_{2,\mathrm{int}} - R^{\mathrm{B}}_{2,\mathrm{int}}) + k_{\mathrm{AB}}$, depends on the difference in intrinsic transverse relaxation rates between ground and excited states. When $R^{\mathrm{A}}_{2,\mathrm{int}} \neq R^{\mathrm{B}}_{2,\mathrm{int}}$ each proton spin-state selective $R_{2,\mathrm{ex}}$ profile will be different because $R_{2,\mathrm{int}}$ values vary for each ^{13}C line in a methyl quartet, Figure 1d. For example, in the limit where only ^{1}H−^{13}C dipolar interactions are considered and for a methyl group attached to a macromolecule with infinitely fast spinning, it has been shown previously that the outer lines relax with rates that are nine times larger than the inner lines.[38−40] *The fact that four distinct dispersion profiles can be recorded and that the $R_{2,int}$ values for each line can be rigorously quantified in terms of a small number of shared parameters (see below), allows the separation of $R^A_{2,int} - R^B_{2,int}$ from k_{AB}.* Indeed, "standard" dispersion profiles that are comprised of the sum of all multiplet components are also sensitive to $R^{\mathrm{A}}_{2,\mathrm{int}} - R^{\mathrm{B}}_{2,\mathrm{int}}$, as has been described by Ishima and Torchia,[34] but it will not be possible in general to separate differences in intrinsic relaxation rates from exchange parameters unless individual multiplet components are considered, as described here.

The decay rates for each of the four methyl carbon transitions can be evaluated, including the proton-carbon dipolar, proton−proton dipolar and the carbon chemical shift anisotropy (CSA) interactions that are the primary sources of relaxation. The derivation, although lengthy, follows standard Redfield theory[41]and similar calculations including contributions from only dipolar interactions have been presented previously.[38,40] We have found it easiest to evaluate the many commutator relations involved using home-written Mathematica (Wolfram Research) or Matlab (MathWorks Inc.) scripts that are available directly from the authors upon request. The intrinsic transverse relaxation rates of the four multiplet components are given by

$$
\begin{aligned}
R^{\mathrm{A},\alpha\alpha\alpha}_{2,\mathrm{int}} &\approx \frac{1}{20}\{2c_{\mathrm{C}} - 3d_{\mathrm{CH}}P_2^0(\cos\theta)\}^2(4J^{\mathrm{A}}(0) + 3J^{\mathrm{A}}(\omega_{\mathrm{C}})) \\
&+ \left\{\frac{1}{2}d^2_{\mathrm{CH}}P_2^1(\cos\theta)^2 + \frac{1}{8}d^2_{\mathrm{CH}}P_2^2(\cos\theta)^2 + \frac{27}{16}d^2_{\mathrm{HH}}\right\}\tau^{\mathrm{A}}_{\mathrm{methyl}} \\
R^{\mathrm{A},\alpha\alpha\beta}_{2,\mathrm{int}} &\approx \frac{1}{20}\{2c_{\mathrm{C}} - d_{\mathrm{CH}}P_2^0(\cos\theta)\}^2(4J^{\mathrm{A}}(0) + 3J^{\mathrm{A}}(\omega_{\mathrm{C}})) \\
&+ \left\{\frac{29}{30}d^2_{\mathrm{CH}}P_2^1(\cos\theta)^2 + \frac{29}{120}d^2_{\mathrm{CH}}P_2^2(\cos\theta)^2 + \frac{99}{80}d^2_{\mathrm{HH}}\right\}\tau^{\mathrm{A}}_{\mathrm{methyl}} \\
R^{\mathrm{A},\alpha\beta\beta}_{2,\mathrm{int}} &\approx \frac{1}{20}\{2c_{\mathrm{C}} + d_{\mathrm{CH}}P_2^0(\cos\theta)\}^2(4J^{\mathrm{A}}(0) + 3J^{\mathrm{A}}(\omega_{\mathrm{C}})) \\
&+ \left\{\frac{29}{30}d^2_{\mathrm{CH}}P_2^1(\cos\theta)^2 + \frac{29}{120}d^2_{\mathrm{CH}}P_2^2(\cos\theta)^2 + \frac{99}{80}d^2_{\mathrm{HH}}\right\}\tau^{\mathrm{A}}_{\mathrm{methyl}} \\
R^{\mathrm{A},\beta\beta\beta}_{2,\mathrm{int}} &\approx \frac{1}{20}\{2c_{\mathrm{C}} + 3d_{\mathrm{CH}}P_2^0(\cos\theta)\}^2(4J^{\mathrm{A}}(0) + 3J^{\mathrm{A}}(\omega_{\mathrm{C}})) \\
&+ \left\{\frac{1}{2}d^2_{\mathrm{CH}}P_2^1(\cos\theta)^2 + \frac{1}{8}d^2_{\mathrm{CH}}P_2^2(\cos\theta)^2 + \frac{27}{16}d^2_{\mathrm{HH}}\right\}\tau^{\mathrm{A}}_{\mathrm{methyl}}
\end{aligned}
\tag{1}
$$

In eq 1, $\tau^{\mathrm{A}}_{\mathrm{methyl}}$ is the correlation time describing rotation about the methyl 3-fold axis in state A, $J^{\mathrm{A}}(\omega)$ is the spectral density function that describes the dynamics of the methyl symmetry axis for state A, ω_{C} is the carbon Larmor frequency, $P_2^0(\cos z) = (3\cos^2 z - 1)/2$, $P_2^1(\cos z) = -3\sin z\cos z$, $P_2^2(\cos z) = 3\sin^2 z$, d_{CH}, d_{HH} and c_{C} are constants given by $d_{\mathrm{CH}} = \gamma_{\mathrm{H}}\gamma_{\mathrm{C}}\hbar\mu_0/(4\pi r^3_{\mathrm{CH}})$, $d_{\mathrm{HH}} = \gamma^2_{\mathrm{H}}\hbar\mu_0/(4\pi r^3_{\mathrm{HH}})$, $c_{\mathrm{C}} = \gamma_{\mathrm{C}}B_0\Delta\sigma/3$ where γ_i is the gyromagnetic ratio for spin i, $\hbar$ is Planck's constant/2π, r_{ij} is the distance between spins i and j, B_0 is the strength of the static magnetic field, and $\Delta\sigma = \sigma_{\parallel} - \sigma_{\perp}$, where $\sigma_{\parallel}$ and $\sigma_{\perp}$ are the components of the assumed axially symmetric methyl ^{13}C chemical shift tensor. The spectral density function is[36]

(38) Kay, L. E.; Bull, T. E. *J. Magn. Reson.* **1992**, *99*, 615–622.
(39) Werbelow, L. G.; Grant, D. M. *Adv. Magn. Reson.* **1977**, *9*, 189–299.
(40) Kay, L. E.; Torchia, D. A. *J. Magn. Reson.* **1991**, *95*, 536–547.
(41) Redfield, A. G. *IBM J. Res. Dev.* **1957**, *1*, 1–19.

$$J^A(\omega) = S^{2,A}_{axis}\frac{\tau^A_C}{1+(\omega\tau^A_C)^2} + (1-S^{2,A}_{axis})\frac{\tau^A_1}{1+(\omega\tau^A_1)^2},$$
$$\frac{1}{\tau^A_1} = \frac{1}{\tau^A_C} + \frac{1}{\tau^A_{axis}} \quad (2)$$

with τ^A_C and τ^A_{axis} correlation times for the overall tumbling and the motion of the methyl symmetry axis (state A), respectively. Analogous equations for state B can be readily obtained by interchanging A and B in the expressions above. In the derivation of eq 1 we have assumed the Woessner model for methyl dynamics,[42] whereby each C−H vector of the methyl group jumps rapidly between three equally probable orientations (τ_{methyl}), with additional motion of the methyl axis relative to a fixed molecular frame on a separate time-scale, τ_{axis} (for example, see eq 15 of ref 40 where such a model is described in more detail, including the effects of cross-correlations). In addition we have retained only the dominant $J(0)$ and $J(\omega_C)$ spectral density terms. While there are additional terms proportional to $J(\omega_H)$, $J(2\omega_H)$ and $J(\omega_H \pm \omega_C)$ their contributions are small. For example, for a small protein with $\tau_C = 4$ ns, $S^2_{axis} = 0.5$, $\tau_{axis} = 300$ ps, $\tau_{methyl} = 50$ ps the combined contributions to the transverse relaxation rates of eq 1 from the $J(\omega_H)$, $J(2\omega_H)$ and $J(\omega_H \pm \omega_C)$ spectral densities are less than 13% of those from the leading terms in eq 1 (8% for $R_2^{\alpha\alpha\alpha}$, 10% for $R_2^{\alpha\alpha\beta}$, 13% for $R_2^{\alpha\beta\beta}$, and 12% for $R_2^{\beta\beta\beta}$). Moreover, in the case where $\tau_C = 1$ ns, $S^2_{axis} = 0.2$, $\tau_{axis} = 300$ ps, $\tau_{methyl} = 50$ ps, $J(\omega_H)$, $J(2\omega_H)$ and $J(\omega_H \pm \omega_C)$ contribute 19% of the total rate (for $R_2^{\beta\beta\beta}$, which is the worse case). A further issue that merits discussion is the validity of the motional model, in particular for applications to excited states that are partially unfolded (or totally unfolded, as in the example here, see below). Is it realistic to assume that the dynamics of methyl containing side-chains in unfolded states can be adequately described assuming that the motion of the $^{13}C-^{1}H$ bond vector is given by a correlation function that decays rapidly to a plateau value $P_2^0(\cos\theta)^2$with correlation time τ_{methyl}, and then more gradually with a rate $1/\tau_{axis}$ to a plateau of $P_2^0(\cos\theta)^2 S^2_{axis}$, before finally decaying to zero due to tumbling with an effective correlation time τ_C? It is unclear whether there is a definitive answer to this question at this time, but some insight can be provided by our previous studies of methyl group dynamics in Δ131Δ, a large, highly populated, disordered fragment of staphylococcal nuclease.[43] These studies made use of a ^2H relaxation method in which side-chain methyl dynamics properties are quantified through intensities of resolved backbone amide correlations. Four different ^2H spin-relaxation rates were measured, shown to be self-consistent, and subsequently fit to a model that is very similar to what is used in eqs 1 and 2. It was found that fits of the data could be obtained that were largely within experimental error and that more complex models of motion could not be justified on the basis of statistical analyses. Of course, the analysis of Δ131Δ was on a 'visible', unfolded protein rather than the invisible, unfolded conformer that is the object of study here (see below) and for which it is almost certain that the quality of data will be lower than that derived from a visible state. Thus, while the model used presently is most certainly crude, more complex models are not warranted, at least until such time that experiments improve considerably.

It is worth reemphasizing the importance of recording spin-state selective dispersion profiles and analyzing the relaxation dispersions from all lines together since this is a major result of the present work. From eq 1 it follows that $R^{j,\alpha\alpha\alpha}_{2,int} \propto (3P_2^0(\cos\theta)d_{CH} - 2c_C)^2 S^{2,j}_{axis}\tau^j_C$ and $R^{j,\alpha\beta\beta}_{2,int} \propto (P_2^0(\cos\theta)d_{CH} + 2c_C)^2 S^{2,j}_{axis}\tau^j_C$ in the macromolecular limit. Thus, in the slow exchange example considered above, $R^{\alpha\alpha\alpha}_{2,ex}(0) - R^{\alpha\beta\beta}_{2,ex}(0) \propto p_B P_2^g(\cos\theta)d_{CH}\{d_{CH}P_2^g(\cos\theta) - 2c_C\}(S^{2,A}_{axis}\tau^A_C - S^{2,B}_{axis}\tau^B_C)$ that does not depend on k_{AB} (see Figure S1 of Supporting Information) and the correlation between k_{AB} and intrinsic relaxation rates is broken. Thus, in the case of a two-state exchange process simultaneous analysis of dispersion profiles from the four lines of the methyl quartet allows extraction of k_{AB}, k_{BA}, $\Delta\omega$ that describe the exchange event as well as dynamical parameters $4J^j(0) + 3J^j(\omega_C)$ for each state $j \in (A,B)$. In all fits of dispersion profiles we have assumed that values of τ_{methyl} and $\Delta\sigma$, while methyl group specific, are identical for states A and B. It is worth noting that in many cases $4J^j(0) \gg 3J^j(\omega_C)$, $\tau^j_C \gg \tau^j_{axis}$ so that $4J^j(0) + 3J^j(\omega_C) \approx 4J^j(0) \approx 4S^{2,j}_{axis}\tau^j_C$.

Figure 2 illustrates the spin-state selective methyl ^{13}C relaxation dispersion NMR experiment that was designed for extracting dynamics parameters of methyl groups in invisible, excited protein states. Central to the experiment is the constant-time CPMG element of duration T_{relax} (between *b* and *c*) during which a train of a variable number of ^{13}C refocusing pulses is applied that quenches the effects of chemical exchange. In the absence of the element between points *a* and *b* of the scheme, $^{13}C,^{1}H$ correlations are produced that are separated into a series of four multiplet components in the carbon dimension according to the four possible methyl proton spin states (see above, Figure 1*b*). In practice the overlap in spectra becomes prohibitive even for applications to small proteins and we have therefore made use of an approach developed by Kontaxis and Bax[44] where each of the four multiplet components is separated into individual subspectra. This is achieved by modulating each of the components according to evolution from the one-bond methyl $^{1}H-^{13}C$ scalar coupling (occurring between *a* and *b*) and subsequently taking linear combinations of data sets to produce the appropriate subspectra, as described in the legend to Figure 2.

The extraction of accurate dynamics parameters is predicated on limiting exchange of magnetization between different ^{13}C methyl group multiplet components that potentially can occur during the course of the experiment. Exchange of this type can result from longitudinal relaxation of methyl protons caused by external protons that effectively "flips" the spin-states of the methyl protons (see Materials and Methods, eqs 4 and 5). This process can be minimized extensively through high levels of deuteration and the samples that have been used (see below) are Ile, Leu, Val methyl protonated in an otherwise highly deuterated background. In addition, the effects of spin- flips can be reduced by (1) separating the four multiplet components as described above to achieve a "clean" initial condition at the start of the CPMG element[28] and by (2) including the scheme in the center of the CPMG element (Figure 2) that effectively

(42) Woessner, D. E. *J. Chem. Phys.* **1962**, *36*, 1–4.
(43) Choy, W. Y.; Shortle, D.; Kay, L. E. *J. Am. Chem. Soc.* **2003**, *125*, 1748–1758.
(44) Kontaxis, G.; Bax, A. *J. Biomol. NMR* **2001**, *20*, 77–82.
(45) Shaka, A. J.; Keeler, J.; Frenkiel, T.; Freeman, R. *J. Magn. Reson.* **1983**, *52*, 335–338.
(46) Levitt, M.; Freeman, R. *J. Magn. Reson.* **1978**, *33*, 473–476.
(47) Piotto, M.; Saudek, V.; Sklenar, V. *J. Biomol. NMR* **1992**, *2*, 661–665.
(48) Marion, D.; Ikura, M.; Tschudin, R.; Bax, A. *J. Magn. Reson.* **1989**, *85*, 393–399.

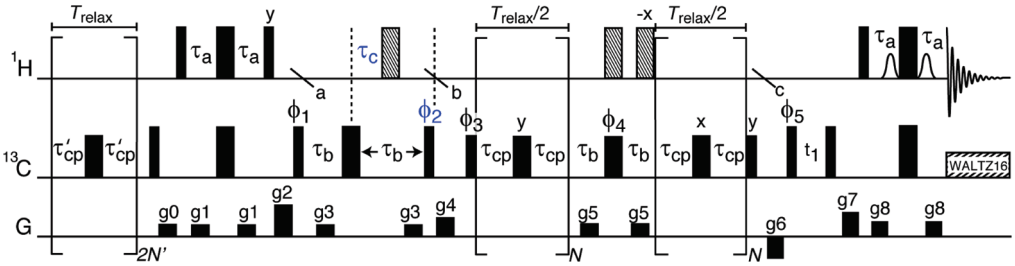

Figure 2. Pulse scheme of the ^{13}C methyl constant-time CPMG relaxation dispersion experiment quantifying methyl dynamics of excited states of proteins. All 90° (180°) radiofrequency pulses are shown as narrow (wide) bars and are applied at the maximum possible power, except for the ^{13}C pulses between *b* and *c* (16 kHz). ^{13}C decoupling is achieved with a 2 kHz WALTZ-16 decoupling field.[45] ^{1}H pulses indicated with shading are applied as $90^\circ_x - 210^\circ_y - 90^\circ_x$ between *a* and *b* and $90^\circ_x - 180^\circ_y - 90^{\circ 46}_x$ between *b* and *c*. The shaped proton pulses applied prior to acquisition are 90° water selective (rectangular) pulses.[47] Phases of rf pulses are x unless explicitly indicated otherwise. Quadrature in F_1 is achieved via States-TPPI[48] of phase $\phi 5$. The delays were set according to: $\tau_a = 1.8$ ms, $\tau_b = 2.0$ ms, $T_{relax} = 50$ ms and N is any whole number between 1 and 50. Gradient levels and durations (Gauss/cm; ms) are: g0 = (4; 0.5), g1 = (5; 0.25), g2 = (25; 1.0), g3 = (4; 0.1), g4 = (6; 1.5), g5 = (5; 0.25), g6 = (−18; 1.5), g7 = (12; 0.3), g8 = (8; 0.5), respectively. The phase cycle is: $\phi 1 = 2(x,-x),2(-x,x)$, $\phi 3 = 2(x),2(-x)$ with $\phi 4 = \{x,-x\}$ to refocus artifacts in dispersion profiles recorded with ^{13}C magnetization coupled to protons in the $\alpha\alpha\alpha$ (most upfield component)/$\alpha\beta\beta$ spin-states or $\phi 4 = \{y,-y\}$ for $\alpha\alpha\beta$, $\beta\beta\beta$, $\phi 5 = 2(x), 2(-x)$, receiver = $\phi 1$. Four separate spectra are recorded in order to separate the multiplet components with $(\tau_c,\phi 2) = (1/(4J_{CH}),x)$, $(1/(6J_{CH}),y)$, $(1/(12J_{CH}),-x)$, and $(0,-y)$ (shown in blue). Postprocessing of these four subspectra yield isolated multiplet components as described previously.[44] In order to keep probe-load as constant as possible a CPMG scheme is applied immediately prior to the start of the sequence where $N' = N_{max} - N$ and $4\tau'_{CP} = T_{relax}/(N_{max} - N)$, and N_{max} is the maximum value of N that is used. The pulse sequence code is available upon request.

'inverts' every second of the four multiplet components,[19,49] described previously in the context of ^{15}N-TROSY based CPMG experiments.[26,50] It is worth noting that depending on the phase of the ^{13}C 180° pulse in this element (*x* or *y*), artifacts that accumulate during the first half of the CPMG train are refocused during the second half for ^{13}C magnetization coupled to protons in the $\alpha\alpha\alpha$, $\alpha\beta\beta$ (phase *x*), or $\alpha\alpha\beta$, $\beta\beta\beta$ (phase *y*) spin states, in a manner analogous to that discussed previously in the context of applications involving spin-state selective ^{15}N dispersions.[26]

Validation—An Application to a Non-Exchanging System. To establish that robust parameters can be extracted from fits of dispersion profiles we first considered an application to a small protein, protein L,[51] which shows evidence of chemical exchange at only a single methyl site (Val 47 C$^{\gamma 1}$, see below). Spin-state selective dispersion data were recorded on a ^{2}H-, Ile-[^{13}CH$_3\delta$1], Leu, Val-[^{13}CH$_3$,^{12}CD$_3$]-labeled sample at a single magnetic field (corresponding to a ^{1}H frequency of 800 MHz); the four dispersion profiles for each residue were constant ($R_{2,\mathrm{eff}}(\nu_{CPMG}) = R^k_{2,\mathrm{int}}$, $k \in \{\alpha\alpha\alpha,\alpha\alpha\beta,\alpha\beta\beta,\beta\beta\beta\}$), as expected, with the exception of those for Val 47 C$^{\gamma 1}$ which showed very slight dependencies on ν_{CPMG}. From the four $R^k_{2,\mathrm{int}}$ rates, values of $(4J(0) + 3J(\omega_C))/4$ and $\Delta\sigma$ were extracted for each methyl group and compared with values isolated from independent experiments. Figure 3a plots $(4J(0) + 3J(\omega_C))/4$ calculated from dynamics parameters measured independently from ^{2}H spin relaxation experiments performed on a fractionally deuterated protein L sample[52] vs corresponding values that were obtained from fits of the dispersion profiles (see Materials and Methods for details); the best fit line through the data is $y = 1.034\ x$ with the one outlier from residue Val 47 C$^{\gamma 1}$ due to chemical exchange that was not taken into account in the analysis. Figure 3*b* plots the ^{1}H−^{13}C dipolar/^{13}C chemical shift anisotropy cross-correlated spin relaxation rate, $\eta_C = 1.46 \times 10^7 \Delta\sigma[(4J(0) + 3J(\omega_C))/4]$ at 800 MHz, measured from the asymmetry of the

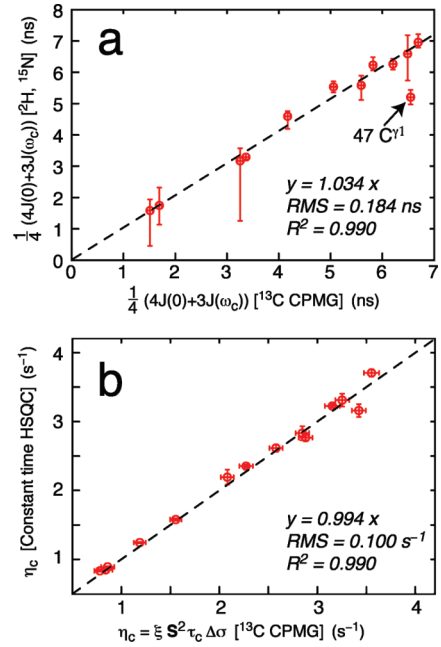

Figure 3. Validation of the methodology using protein L. (a) Correlation between $(4J(0) + 3J(\omega_C))/4$ values (5 °C) calculated from dynamics parameters based on ^{2}H spin-relaxation[52] (Y-axis) and from ^{13}C CPMG relaxation dispersion profiles (*x*-axis; measured at 800 MHz). Values derived from CPMG relaxation dispersions were multiplied by 0.805[54] to take into account differences in viscosity between 100% D_2O (sample for ^{13}C CPMG) and 90% H_2O/10% D_2O (sample for ^{2}H spin relaxation). Val 47 C$^{\gamma 1}$ undergoes millisecond chemical exchange and was therefore excluded from calculation of the best-fit line, rms, and R^2. (b) Correlation between ^{1}H−^{13}C dipolar/^{13}C chemical shift anisotropy cross-correlated spin relaxation rates, η_C, 800 MHz, 5 °C, measured using the method of Tugarinov and Kay (*y*-axis)[53] and using the CPMG method (X-axis), as described in the text. The proportionality factor $\xi = 1.46 \times 10^7$ 1/ppm.

intensities of methyl ^{13}C multiplet components in coupled HSQC spectra (Y-axis)[53] and the corresponding values calculated based on parameters extracted from fits of the dispersion profiles (*x*-axis). The good agreement observed in Figures 3*a* and 3*b* suggests that accurate dynamics parameters can be extracted

(49) Skrynnikov, N. R.; Mulder, F. A. A.; Hon, B.; Dahlquist, F. W.; Kay, L. E. *J. Am. Chem. Soc.* **2001**, *123*, 4556–4566.
(50) Loria, J. P.; Rance, M.; Palmer, A. G. *J. Biomol. NMR* **1999**, *15*, 151–155.
(51) Scalley, M. L.; Yi, Q.; Gu, H.; McCormack, A.; Yates, J. R.; Baker, D. *Biochemistry* **1997**, *36*, 3373–3382.
(52) Skrynnikov, N. R.; Millet, O.; Kay, L. E. *J. Am. Chem. Soc.* **2002**, *124*, 6449–6460.
(53) Tugarinov, V.; Kay, L. E. *J. Biomol. NMR* **2004**, *29*, 369–376.

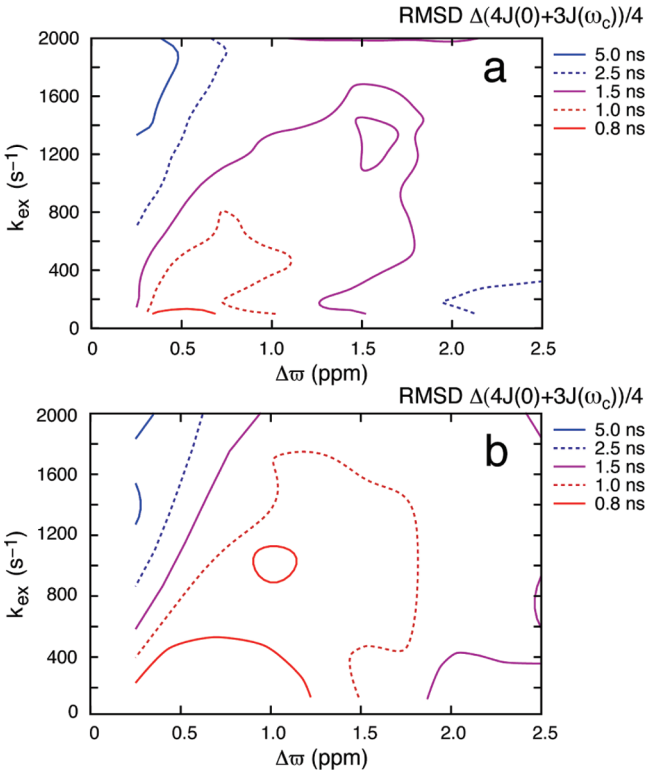

Figure 4. Predicted uncertainties in extracted values of $\Delta(4J(0) + 3J(\omega_C))/4 = (4J^A(0) + 3J^A(\omega_C))/4 - (4J^B(0) + 3J^B(\omega_C))/4$ as a function of k_{ex} (y-axis) and $\Delta\varpi$ (x-axis). Values of $p_B = 3\%$ (A) and 5% (B) are chosen with other parameters given in the text.

from the CPMG method using the relaxation model described in Materials and Methods (see below).

Sensitivity to Chemical Shift Time-Scale. Having established that accurate motional parameters of the ground state can be extracted from fits of dispersion profiles in the absence of exchange we next consider the case of chemical exchange and investigate how the fitted dynamics parameters depend on the chemical exchange time-scale. This is addressed through computations in which a set of spin-state selective dispersion profiles corresponding to the evolution of each of $\mathbf{C}_{+}^{\alpha\alpha\alpha}$, $\mathbf{C}_{+}^{\alpha\alpha\beta}$, $\mathbf{C}_{+}^{\alpha\beta\beta}$, and $\mathbf{C}_{+}^{\beta\beta\beta}$ were generated at 600 and 800 MHz using experimental ν_{CPMG} values along with the parameters $\Delta(4J(0) + 3J(\omega_C))/4 = (4J^A(0) + 3J^A(\omega_C))/4 - (4J^B(0) + 3J^B(\omega_C))/4 = 2$ ns, $\Delta\sigma = 25$ ppm, $(4J^A(0) + 3J^A(\omega_C))/4 = 4$ ns, $J_{CH} = 125$ Hz, $\tau_{methyl} = 50$ ps for 100 $s^{-1} \le k_{ex} \le 2000$ s^{-1} (varied in steps of 76 s^{-1}) and 0.25 ppm $\le |\Delta\varpi| \le 2.5$ ppm (steps of 0.09 ppm). From each of these 'parent' data sets 32 additional data sets were obtained by adding Gaussian noise to the parent, with the standard deviation of the Gaussian noise given by the relation 0.15 s^{-1} + 0.16 $s^{-1}ppm^{-1}|\Delta\varpi|$, as estimated from the experimental data. Each of the 32 noise containing data sets (noise added to mimic experimental data) was analyzed independently following the same procedure used for the experimental data to produce 32 values of $\Delta(4J(0) + 3J(\omega_C))/4$ from which a mean and rmsd was calculated. Figure 4 plots the rmsd values for $p_B = 3$ (Figure 4a) and 5% (Figure 4b). It is clear that unreliable values of $\Delta(4J(0) + 3J(\omega_C))/4$ and hence of $(4J^B(0) + 3J^B(\omega_C))/4$ are obtained toward the fast exchange regime ($\Delta\varpi/k_{ex} \rightarrow 0$). Interestingly, in cases for which $\Delta\varpi$ values are large the errors increase as well, reflecting the larger uncertainties in $R_{2,eff}$ and the fact that it is not possible to properly "pulse-out" the exchange contributions using the ν_{CPMG} fields employed experimentally ($\le 1-1.5$ kHz) so that at the highest ν_{CPMG} value the fast pulsing limit is not achieved and therefore $R_{2,eff} \neq p_A R^A_{2,int} + p_B R^B_{2,int}$. Figure 4 also makes clear that significant rmsd values (on the order of 1 ns or larger) are obtained in general, reflecting the fact that the dynamics information derives from differences in multiplet selective dispersion profiles that are often quite small (see below). Nevertheless, in the example of protein folding considered below $p_B \approx 4-5\%$, $k_{ex} \approx 250$ s^{-1} and Figure 4b establishes that reasonably accurate values of $\Delta(4J(0) + 3J(\omega_C))/4$ can be obtained.

We have also examined the effects of dynamic frequency shifts and magnetic field induced molecular alignment on extracted motional parameters and these are shown to be small (see Supporting Information).

Application to Protein Folding. In the previous sections results from experiments have been presented showing that accurate motional parameters can be extracted from fits of dispersion profiles in the absence of exchange and simulations have established guidelines for when quantification of spin-state selective dispersion profiles gives accurate motional parameters in the case of an exchanging system. We now turn to an application involving a G48M mutant of the Fyn SH3 domain that exchanges between folded (ground state) and unfolded (invisible excited state) conformers. Previous studies have shown that the fractional population of the unfolded state, p_U, is 3.5% at 23 °C and that the folding reaction proceeds via an on-pathway intermediate state whose population p_I is 0.7%.[55] In the analysis that follows we have assumed that the folding/unfolding exchange process for this protein can be modeled as two-state since $p_I < p_U$; fits of dispersion profiles on a per-residue basis produced exchange rate constants for k_{AB} (k_{BA}) that varied by less than 10%(20%) from the mean value, Tables S1, S2 of Supporting Information, much less than the 10−100 fold differences that were noted in previous studies of folding where intermediates were formed with similar populations to the unfolded state.[10,56]

A ^{2}H-, Ile-[$^{13}CH_3\delta1$], Leu, Val-[$^{13}CH_3$,$^{13}CH_3$]-labeled sample of G48M Fyn SH3 was produced and dispersion profiles recorded using the scheme of Figure 2. Figure 5a shows one such set of profiles from each of the four multiplet components of Leu 7 $C^{\delta2}$ recorded at 23 °C, 800 MHz (squares) that are analyzed with a two-site-exchange model (solid lines) described in detail in Materials and Methods. Notably, small but significant differences in spin-state selective profiles are obtained, Figure 5b, which provide the telltale sign that the intrinsic ps-ns time-scale dynamics in the two exchanging states are distinct. As further support for an exchange model which includes differential dynamics between ground and excited states, p-values have been calculated to evaluate the statistical significance of including separate relaxation rates for each of the two states (Figure S3, Supporting Information). For those residues where differences in dynamics are small, large p-values are obtained as expected, indicating that the more complex fitting model (differential dynamics) is unnecessary. However, $p < 0.031$ for all cases where $\Delta(4J(0) + 3J(\omega_C))/4 > 1.5$ ns (see Supporting

(54) Cho, C. H.; Urquidi, J.; Singh, S.; Robinson, G. W. *J. Phys. Chem. B.* **1999**, *103*, 1991–1994.
(55) Mittermaier, A.; Korzhnev, D. M.; Kay, L. E. *Biochemistry* **2005**, *44*, 15430–15436.
(56) Korzhnev, D. M.; Neudecker, P.; Zarrine-Afsar, A.; Davidson, A. R.; Kay, L. E. *Biochemistry* **2006**, *45*, 10175–10183.

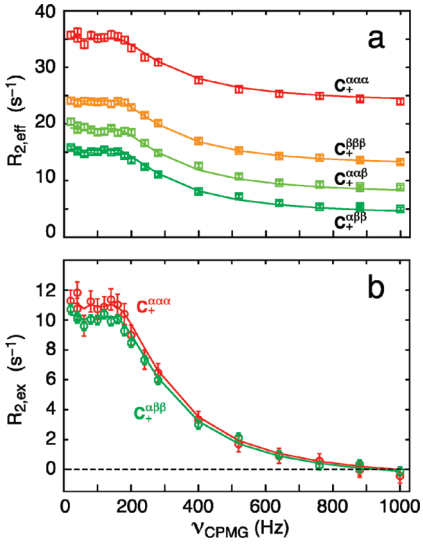

Figure 5. Spin-state selective relaxation dispersion profiles. (a) Methyl CPMG relaxation dispersion profiles of Leu 7 $C^{\delta 2}$ from the G48M Fyn SH3 domain, 500 mM GdnHCl, recorded at 800 MHz, 23 °C, using the pulse sequence of Figure 2. (b) Contribution to $R_{2,eff}$ from the chemical exchange process, $R_{2,ex} = R_{2,eff}(\nu_{CPMG}) - \lim_{\nu_{CPMG}\to\infty} R_{2,eff}(\nu_{CPMG})$. The difference between $R_{2,ex}(\mathbf{C}_+^{\alpha\alpha\alpha})$ and $R_{2,ex}(\mathbf{C}_+^{\alpha\beta\beta})$ reports directly on the dynamics of the excited state. In this example, $R_{2,ex}(\mathbf{C}_+^{\alpha\alpha\alpha}) > R_{2,ex}(\mathbf{C}_+^{\alpha\beta\beta})$, so that $S_A^2 > S_B^2$ for Leu 7 $C^{\delta 2}$.

Information). Notably, a p-value of 1.1×10^{-5} is obtained from fits of dispersion profiles for Leu 7$C^{\delta 2}$, consistent with expectations. In contrast, as described in the first section of Results and Discussion, and emphasized in a previous publication by Ishima and Torchia,[34] if single-quantum dispersion data sets quantifying the decay of the total transverse magnetization were to be recorded and analyzed (nonspin state selective experiments) it would not be possible to distinguish between models which assume identical motional properties between ground and excited states and those with different ps-ns time-scale dynamics. It is thus critical that individual multiplet components be studied.

Figure 6a plots $(4J(0) + 3J(\omega_C))/4 \approx S^2_{axis}\tau_C$ for the folded (blue circles) and invisible, unfolded (red circles) states of the G48M Fyn SH3 domain, 23 °C, averaged over measurements for $C^{\delta 1}$,$C^{\delta 2}$ ($C^{\gamma 1}$,$C^{\gamma 2}$) in the case of Leu (Val) residues. $S^{2,B}_{axis}\tau^B_C$ values (excited state) for each methyl group are indicated by triangles ($\delta 1/\gamma 1$) and squares ($\delta 2/\gamma 2$) displaced slightly from each other for Leu and Val and by triangles for Ile. All but one of the 16 Ile, Leu and Val methyl groups in the protein could be reliably quantified; $\Delta\varpi$ of Ile28 $C^{\delta 1}$ is so large (2.8 ppm) that its dispersion profile could not be fully quenched using the ν_{CPMG} values of the experiment, leading to large uncertainties in the fitted parameters. Not surprisingly, $R^A_{2,int} \geq R^B_{2,int}$, indicating that the unfolded state ensemble is more dynamic than the folded conformation on the ps-ns time-scale. Interestingly, methyl groups at the C-terminal end of the excited state are less dynamic than in other regions of the protein. This asymmetry of motion (as a function of sequence) suggests that the unfolded state for the G48M Fyn SH3 domain is not completely random-coil like. With the exception of the values at the C-terminus, the $S^{2,B}_{axis}\tau^B_C$ values obtained here are similar to those measured for methyl groups in Δ131Δ, studied by a ^{2}H relaxation method described briefly above and in detail previously.[43]

As a follow-up experiment we were interested in examining how small quantities of GdnHCl (500 mM) might affect the dynamic properties of the side-chain Ile, Leu, Val residues in both folded and unfolded conformations. In particular, is a

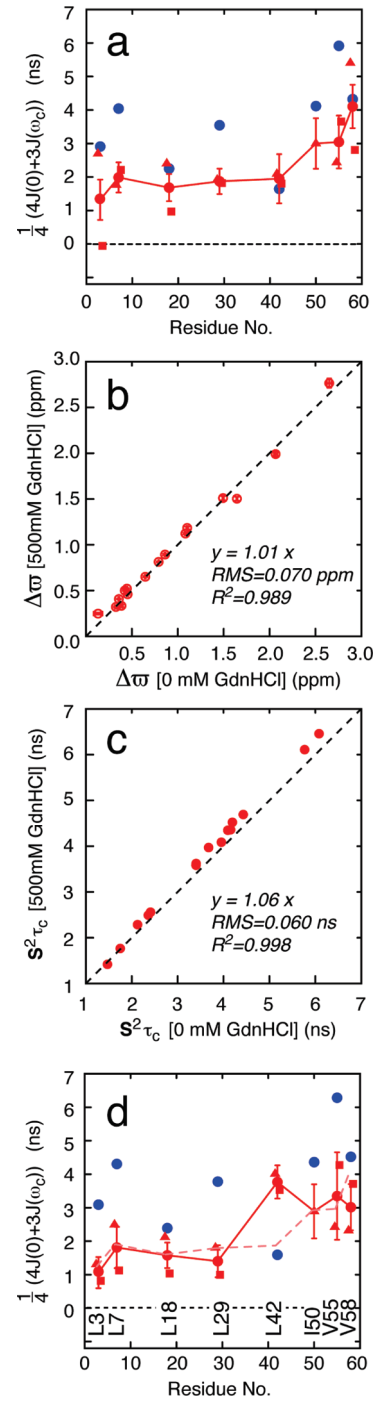

Figure 6. (a) Methyl axis dynamics, $(4J(0) + 3J(\omega_C))/4 \approx S^2_{axis}\tau_C$, of the ground (blue filled circles) and excited (red circles and red line) G48M Fyn SH3 domain states derived from CPMG relaxation dispersion, 23 °C. For Val (Leu) residues the values for $C^{\gamma 1}$, $C^{\gamma 2}$ ($C^{\delta 1}$, $C^{\delta 2}$) are shown to the left (▲), right (□) of the average value (●), with the vertical bars indicating the uncertainty in the average. (b) Differences in chemical shifts, $\Delta\varpi$ (ppm), between ground (folded) and excited (unfolded) states of the G48M Fyn SH3 domain measured in the presence (y-axis) and absence (x-axis) of 500 mM GdnHCl. (c) Values of $(4J^A(0) + 3J^A(\omega_C))/4 \approx S^{2,A}_{axis}\tau^A_C$ measured for samples with and without GdnHCl. (d) Same as in (a), except with 500 mM GdnHCl. The dotted red line is the continuous red curve from (a).

similar dynamics profile to that illustrated in Figure 6a for the unfolded domain also observed in the presence of 500 mM denaturant, or does the added GdnHCl result in increased motion at the C-terminal end of the protein, due presumably to a "melting" of some stabilizing interaction in the unfolded state?

As expected, the addition of GdnHCl stabilized the excited state with p_U increasing from 4.3 ± 0.7 to 5.4 ± 0.9% and k_{ex}, that reflects largely the folding rate, decreasing from 305 ± 40 to 237 ± 49 s^{-1}. Fits of spin-state selective dispersion profiles establish that the ^{13}C methyl $\Delta\varpi$ values for Ile, Leu, Val residues are not changed upon the addition of 500 mM GdnHCl, Figure 6b (slope of the $\Delta\varpi$ correlation is 1.01). In addition, the chemical shift changes in the ground state are very minor (0.033 ± 0.059 ppm on average), establishing that the methyl shifts in the unfolded state are not perturbed through the addition of GdnHCl and hence very likely neither is the 'average unfolded structure'. Moreover, the relative ps-ns time-scale methyl dynamics of the ground state ($(4J^A(0) + 3J^A(\omega_C))/4 \approx S^{2,A}_{axis}\tau^A_C$) are not changed upon addition of GdnHCl (Figure 6c). The best-fit line through the linear correlation plot is $y = 1.06x$, with the overall increase in transverse relaxation (6%) most likely reflecting a slight increase in solution viscosity associated with the addition of GdnHCl. Figure 6d plots ground (blue) and excited (red) state dynamical parameters that are measured in the presence of 500 mM GdnHCl. The dashed red line shows the values for the excited state in the absence of GdnHCl (Figure 6a) for comparison. As observed with the ground state, rather similar $S^{2,B}_{axis}\tau^B_C$ values are obtained with and without GdnHCl for residues of the unfolded polypeptide chain, with the exception of Leu 42 whose motion becomes much more restricted in the presence of denaturant (note that both $C^{\delta1}$,$C^{\delta2}$ positions of Leu 42 have very similar dynamics parameters), indicating perhaps some stabilizing interaction at this position. Notably, if weak and transient hydrophobic interactions underlie the rigidity at the carboxy-terminal end of the excited state, Figure 6a, then the results of the present study indicate that the addition of small amounts of GdnHCl are not able to disrupt them.

In summary, a method is presented for the measurement of methyl group motional parameters of invisible, excited protein states using ^1H spin-state selective relaxation dispersion NMR spectroscopy. The present work complements previous studies where parameters reporting on the structure of the excited state were measured.[29] The predicted uncertainties in dynamics parameters of the excited state (Figure 4) and the experimental uncertainties (Figure 6, Tables S1b, S2b, Supporting Information) indicate that, despite the fact that accurate spin state selective dispersion profiles can be recorded, the fidelity of the extracted excited state parameters are compromised by the small effects of differential ps−ns dynamics on the resulting dispersion profiles. Nevertheless, significant changes in dynamics parameters as a function of sequence for the unfolded state of the G48M Fyn SH3 domain have been obtained unequivocally from the present study. It is thus clear on the basis of these results that a particular strength of the methodology will be in studies of folding intermediates where a qualitative site-specific indication of formation of structural contacts in the excited (partially folded) state can be obtained, based on how the dynamics in ground and excited conformers compare. It is also clear that relaxation dispersion spectroscopy is emerging as an important tool for the characterization of invisible, excited state conformations at a level of detail that is at least starting to approach that normally restricted to applications involving visible, ground states of proteins.

Materials and Methods

Sample Preparation. A ^2H-, Ile-[$^{13}CH_3\delta1$], Leu, Val-[$^{13}CH_3$,$^{13}CH_3$]-labeled sample of the G48M Fyn SH3 domain was expressed and purified as described previously.[55] The protein concentration was ≈1 mM, and the sample contained 50 mM sodium phosphate, 1 mM EDTA, 1 mM NaN_3, 90%/10% H_2O/D_2O, pH 7.0; a second sample was prepared by adding guanidine hydrochloride (GdnHCl) to a concentration of 500 mM. A 1.2 mM sample of ^2H-, Ile-[$^{13}CH_3\delta1$], Leu, Val-[$^{13}CH_3$,$^{12}CD_3$]-protein L, 99.9% D_2O, 50 mM sodium phosphate, pH 6.0, prepared as discussed previously,[53] was used as a test-sample in some of the experiments.

NMR Spectroscopy and Data Analysis. Four constant-time ^{13}C-methyl CPMG relaxation dispersion experiments, corresponding to the four values of (τ_C,ϕ_2) in Figure 2, were recorded at 23 °C and at three static magnetic fields strengths corresponding to ^1H resonance frequencies of 600 (cryogenically cooled probe-head) and 500, 800 (room temperature probe-head) MHz (no GdnHCl) or at two magnetic fields, 600 and 800 MHz (with GdnHCl). Spectra of the four ^{13}C multiplet components were separated as described by Kontaxis and Bax.[44] Subsequently, relaxation dispersion profiles, $R_{2,eff}(\nu_{CPMG})$, for each of the components were generated from peak intensities, $I_1(\nu_{CPMG})$, in a series of 2D $^1H-^{13}C$ correlation maps measured as a function of CPMG frequency, $\nu_{CPMG} = 1/(4\tau_{CP})$, where $2\tau_{CP}$ is the interval between consecutive refocusing pulses of the CPMG sequence. Peak intensities were converted into effective relaxation rates via $R_{2,eff}(\nu_{CPMG}) = \ln(I_0/I_1(\nu_{CPMG}))/T_{relax}$, where I_0 is the peak intensity in a reference spectrum recorded without the relaxation delay T_{relax}.[57] Dispersion profiles were recorded with $T_{relax} = 50$ ms and 22 (26) values of ν_{CPMG} ranging from 25 to 1000 Hz, along with 2 repeats for error analysis at static magnetic fields corresponding to ^1H resonance frequencies of 600 and 800 MHz for the sample with (without) GdnHCl. For the sample without GdnHCl an additional dispersion data set was recorded at 500 MHz. Values of R^A_{sel} (see below) were calculated by measuring the relaxation rates $R_1(4C_ZH^i_ZH^j_Z)$, $R_1(2C_ZH^i_Z)$ of individual methyl groups encoded in the intensities of cross-peaks in 2D $^{13}C-^1H$ correlation maps (pulse sequences available upon request). The decay times used to measure the R_1 values ranged from 3 to 150 ms.

Data sets were processed and analyzed with the NMRPipe program[58] and signal intensities were quantified using the program FuDA (http://pound.med.utoronto.ca/software.html). Relaxation dispersion data were interpreted using a 2-state exchange model,

$$A \underset{k_{BA}}{\overset{k_{AB}}{\rightleftharpoons}} B$$

with 8 or 12 spin-state selective dispersion profiles from each methyl (four each at 600 and 800 MHz or 500, 600, and 800 MHz) analyzed simultaneously. The best-fit model parameters were extracted using the program CATIA which is available from http://pound.med.utoronto.ca/software.html and which has been described previously.[26] Briefly, parameters are obtained by minimization of the target function,

(57) Mulder, F. A. A.; Skrynnikov, N. R.; Hon, B.; Dahlquist, F. W.; Kay, L. E. *J. Am. Chem. Soc.* **2001**, *123*, 967–975.
(58) Delaglio, F.; Grzesiek, S.; Vuister, G. W.; Zhu, G.; Pfeifer, J.; Bax, A. *J. Biomol. NMR* **1995**, *6*, 277–293.
(59) McConnell, H. M. *J. Chem. Phys.* **1958**, *28*, 430–431.

$$\chi^2(\zeta) = \sum \frac{(R_{2,\mathrm{eff}}^{\mathrm{clc}}(\zeta) - R_{2,\mathrm{eff}}^{\mathrm{exp}})^2}{(\Delta R_{2,\mathrm{eff}}^{\mathrm{exp}})^2} \tag{3}$$

where $R_{2,\mathrm{eff}}^{\mathrm{exp}}$ and $\Delta R_{2,\mathrm{eff}}^{\mathrm{exp}}$ are experimental effective relaxation rates and their uncertainties, respectively, $R_{2,\mathrm{eff}}^{\mathrm{clc}}(\zeta)$ are calculated relaxation rates obtained by numerical integration of the Bloch-McConnell equations,[59] $\zeta = \{x_1, ..., x_{npar}\}$ denotes the set of adjustable model parameters and the summation is over the number of experimental data points.

Model of Two-Site Chemical Exchange.

As described in the text, the ^{13}C spin of a methyl group is scalar coupled to its three directly attached protons with scalar coupling constant J_{CH}, giving rise to four distinct carbon transitions in NMR spectra. The four lines are denoted as $\mathbf{C}_+^{\alpha\alpha\alpha}$, $\mathbf{C}_+^{\alpha\alpha\beta}$, $\mathbf{C}_+^{\alpha\beta\beta}$, and $\mathbf{C}_+^{\beta\beta\beta}$ where $\mathbf{C}_+^{\alpha\alpha\alpha} = \mathbf{C}_+\mathbf{H}_1{}^{|\alpha\rangle}\mathbf{H}_2{}^{|\alpha\rangle}\mathbf{H}_3{}^{|\alpha\rangle}$, $\mathbf{C}_+^{\alpha\alpha\beta} = \mathbf{C}_+\mathbf{H}_1{}^{|\alpha\rangle}\mathbf{H}_2{}^{|\alpha\rangle}\mathbf{H}_3{}^{|\beta\rangle} + \mathbf{C}_+\mathbf{H}_1{}^{|\alpha\rangle}\mathbf{H}_2{}^{|\beta\rangle}\mathbf{H}_3{}^{|\alpha\rangle} + \mathbf{C}_+\mathbf{H}_1{}^{|\beta\rangle}\mathbf{H}_2{}^{|\alpha\rangle}\mathbf{H}_3{}^{|\alpha\rangle}$, $\mathbf{C}_+^{\alpha\beta\beta} = \mathbf{C}_+\mathbf{H}_1{}^{|\alpha\rangle}\mathbf{H}_2{}^{|\beta\rangle}\mathbf{H}_3{}^{|\beta\rangle} + \mathbf{C}_+\mathbf{H}_1{}^{|\beta\rangle}\mathbf{H}_2{}^{|\alpha\rangle}\mathbf{H}_3{}^{|\beta\rangle} + \mathbf{C}_+\mathbf{H}_1{}^{|\beta\rangle}\mathbf{H}_2{}^{|\beta\rangle}\mathbf{H}_3{}^{|\alpha\rangle}$ and $\mathbf{C}_+^{\beta\beta\beta} = \mathbf{C}_+\mathbf{H}_1{}^{|\beta\rangle}\mathbf{H}_2{}^{|\beta\rangle}\mathbf{H}_3{}^{|\beta\rangle}$ and are centered at the frequencies $\{\omega - 3\pi J_{\mathrm{CH}}, \omega - \pi J_{\mathrm{CH}}, \omega + \pi J_{\mathrm{CH}}, \omega + 3\pi J_{\mathrm{CH}}\}$ with intrinsic transverse relaxation rates of $\{R_{2,\mathrm{int}}^{\alpha\alpha\alpha}, R_{2,\mathrm{int}}^{\alpha\alpha\beta}, R_{2,\mathrm{int}}^{\alpha\beta\beta}, R_{2,\mathrm{int}}^{\beta\beta\beta}\}$. The time-dependence of each of the methyl−carbon magnetization components in the free precession limit can be written as

$$\frac{\mathrm{d}}{\mathrm{d}t}\boldsymbol{\nu} = -\begin{pmatrix} \rho^{\mathrm{A},\alpha\alpha\alpha} & -k_{\mathrm{BA}} & -0.5R_{\mathrm{sel}}^{\mathrm{A}} & 0 & 0 & 0 & 0 & 0 \\ -k_{\mathrm{AB}} & \rho^{\mathrm{B},\alpha\alpha\alpha} & 0 & -0.5R_{\mathrm{sel}}^{\mathrm{B}} & 0 & 0 & 0 & 0 \\ -1.5R_{\mathrm{sel}}^{\mathrm{A}} & 0 & \rho^{\mathrm{A},\alpha\alpha\beta} & -k_{\mathrm{BA}} & -R_{\mathrm{sel}}^{\mathrm{A}} & 0 & 0 & 0 \\ 0 & -1.5R_{\mathrm{sel}}^{\mathrm{B}} & -k_{\mathrm{AB}} & \rho^{\mathrm{B},\alpha\alpha\beta} & 0 & -R_{\mathrm{sel}}^{\mathrm{B}} & 0 & 0 \\ 0 & 0 & -R_{\mathrm{sel}}^{\mathrm{A}} & 0 & \rho^{\mathrm{A},\alpha\beta\beta} & -k_{\mathrm{BA}} & -1.5R_{\mathrm{sel}}^{\mathrm{A}} & 0 \\ 0 & 0 & 0 & -R_{\mathrm{sel}}^{\mathrm{B}} & -k_{\mathrm{AB}} & \rho^{\mathrm{B},\alpha\beta\beta} & 0 & -1.5R_{\mathrm{sel}}^{\mathrm{B}} \\ 0 & 0 & 0 & 0 & -0.5R_{\mathrm{sel}}^{\mathrm{A}} & 0 & \rho^{\mathrm{A},\beta\beta\beta} & -k_{\mathrm{BA}} \\ 0 & 0 & 0 & 0 & 0 & -0.5R_{\mathrm{sel}}^{\mathrm{B}} & -k_{\mathrm{AB}} & \rho^{\mathrm{B},\beta\beta\beta} \end{pmatrix}\boldsymbol{\nu} \tag{4}$$

$$\boldsymbol{\nu} = (\mathbf{C}_+^{\mathbf{A},\alpha\alpha\alpha}, \mathbf{C}_+^{\mathbf{B},\alpha\alpha\alpha}, \mathbf{C}_+^{\mathbf{A},\alpha\alpha\beta}, \mathbf{C}_+^{\mathbf{B},\alpha\alpha\beta}, \mathbf{C}_+^{\mathbf{A},\alpha\beta\beta}, \mathbf{C}_+^{\mathbf{B},\alpha\beta\beta}, \mathbf{C}_+^{\mathbf{A},\beta\beta\beta}, \mathbf{C}_+^{\mathbf{B},\beta\beta\beta})^{\dagger}$$

where

$$\begin{aligned} \rho^{\mathrm{A},\alpha\alpha\alpha} &= R_{2,\mathrm{int}}^{\mathrm{A},\alpha\alpha\alpha} - i(\omega_{\mathrm{A}} - 3\pi J_{\mathrm{CH}}) + k_{\mathrm{AB}} + 1.5R_{\mathrm{sel}}^{\mathrm{A}} \\ \rho^{\mathrm{B},\alpha\alpha\alpha} &= R_{2,\mathrm{int}}^{\mathrm{B},\alpha\alpha\alpha} - i(\omega_{\mathrm{B}} - 3\pi J_{\mathrm{CH}}) + k_{\mathrm{BA}} + 1.5R_{\mathrm{sel}}^{\mathrm{B}} \\ \rho^{\mathrm{A},\alpha\alpha\beta} &= R_{2,\mathrm{int}}^{\mathrm{A},\alpha\alpha\beta} - i(\omega_{\mathrm{A}} - \pi J_{\mathrm{CH}}) + k_{\mathrm{AB}} + 1.5R_{\mathrm{sel}}^{\mathrm{A}} \\ \rho^{\mathrm{B},\alpha\alpha\beta} &= R_{2,\mathrm{int}}^{\mathrm{B},\alpha\alpha\beta} - i(\omega_{\mathrm{B}} - \pi J_{\mathrm{CH}}) + k_{\mathrm{BA}} + 1.5R_{\mathrm{sel}}^{\mathrm{B}} \\ \rho^{\mathrm{A},\alpha\beta\beta} &= R_{2,\mathrm{int}}^{\mathrm{A},\alpha\beta\beta} - i(\omega_{\mathrm{A}} + \pi J_{\mathrm{CH}}) + k_{\mathrm{AB}} + 1.5R_{\mathrm{sel}}^{\mathrm{A}} \\ \rho^{\mathrm{B},\alpha\beta\beta} &= R_{2,\mathrm{int}}^{\mathrm{B},\alpha\beta\beta} - i(\omega_{\mathrm{B}} + \pi J_{\mathrm{CH}}) + k_{\mathrm{BA}} + 1.5R_{\mathrm{sel}}^{\mathrm{B}} \\ \rho^{\mathrm{A},\beta\beta\beta} &= R_{2,\mathrm{int}}^{\mathrm{A},\beta\beta\beta} - i(\omega_{\mathrm{A}} + 3\pi J_{\mathrm{CH}}) + k_{\mathrm{AB}} + 1.5R_{\mathrm{sel}}^{\mathrm{A}} \\ \rho^{\mathrm{B},\beta\beta\beta} &= R_{2,\mathrm{int}}^{\mathrm{B},\beta\beta\beta} - i(\omega_{\mathrm{B}} + 3\pi J_{\mathrm{CH}}) + k_{\mathrm{BA}} + 1.5R_{\mathrm{sel}}^{\mathrm{B}} \end{aligned} \tag{5}$$

the superscript "†" indicates transpose and $R_{2,\mathrm{int}}^{j,k}$, $j \in (A,B)$, $k \in \{\alpha\alpha\alpha, \alpha\alpha\beta, \alpha\beta\beta, \beta\beta\beta\}$ are the intrinsic transverse relaxation rates of each of the multiplet components of state j given in eq 1 and $R_{\mathrm{sel}}^{\mathrm{A}}(R_{\mathrm{sel}}^{\mathrm{B}})$is the selective ^{1}H longitudinal relaxation rate for state A(B) that is given by the difference in relaxation rates between $4C_ZH_Z^iH_Z^j$ and $2C_ZH_Z^i$, $R_{\mathrm{sel}} = R_1(4C_ZH_Z^iH_Z^j) - R_1(2C_ZH_Z^i)$.[47] In general, R_{sel} is proportional to $J(0)$ in studies of biomolecules.[60] Thus, values of R_{sel} which have been measured for the visible state (A) can be used to calculate the corresponding $R_{\mathrm{sel}}^{\mathrm{B}}$ rates determined during fits of the dispersion profiles according to the relation $R_{\mathrm{sel}}^{\mathrm{B}} \approx R_{\mathrm{sel}}^{\mathrm{A}}(4J^{\mathrm{B}}(0) + 3J^{\mathrm{B}}(\omega_{\mathrm{C}}))/(4J^{\mathrm{A}}(0) + 3J^{\mathrm{A}}(\omega_{\mathrm{C}}))$.

Dispersion profiles for each methyl group were analyzed separately. We prefer to analyze the dispersion data on a per-methyl group basis, as opposed to a global fit involving all residues, since small deviations from two-state behavior can be accounted for in per-residue fits by slight shifts in values of k_{AB} and k_{BA}. We observe small differences in kinetic constants from fits of dispersion profiles derived from different residues as detailed in Tables S1 and S2 (see Supporting Information), with $k_{\mathrm{AB}} = 12.4 \pm 1.2\ \mathrm{s}^{-1}$, $k_{\mathrm{BA}} = 294\ \mathrm{s}^{-1} \pm 39\ \mathrm{s}^{-1}$ (average ± rmsd) and $k_{\mathrm{AB}} = 11.8 \pm 1.7\ \mathrm{s}^{-1}$, $k_{\mathrm{BA}} = 225\ \mathrm{s}^{-1} \pm 49\ \mathrm{s}^{-1}$ for the G48M Fyn SH3 domain without and with 500 mM GdnHCl, respectively.

For each fit, values of k_{AB} and k_{BA} (or p_{B}, $k_{\mathrm{ex}} = k_{\mathrm{AB}} + k_{\mathrm{BA}}$) were extracted, along with $\Delta\omega_{\mathrm{AB}}$, $4J^{A}(0) + 3J^{A}(\omega_{\mathrm{C}})$, $4J^{\mathrm{B}}(0) + 3J^{B}(\omega_{\mathrm{C}})$, $\Delta\sigma$ and τ_{methyl}, Tables S1, S2 (Supporting Information). A value of $J_{\mathrm{CH}} = 125$ Hz, that is the same in both ground and excited states, is assumed in all fits. Contributions, including those from fast exchange processes (faster than ~2000/s), were taken into account by adding an extra term, $\Lambda = \alpha B_0{}^2$ to each of the four rates, $R_{2,\mathrm{int}}^{\mathrm{A},\alpha\alpha\alpha}$, $R_{2,\mathrm{int}}^{\mathrm{A},\alpha\alpha\beta}$, $R_{2,\mathrm{int}}^{\mathrm{A},\alpha\beta\beta}$, $R_{2,\mathrm{int}}^{\mathrm{A},\beta\beta\beta}$. In summary, a total of 8 parameters are extracted from fits of at least 8 and often 12 multiplet selective dispersion profiles (4 relaxation curves for each static magnetic field employed).

Values of Λ from fits are in general small, on average $(0.0014 \pm 0.0019)s^{-1}T^{-2} B_0^2$, corresponding to $\sim 0.25\ s^{-1}$ at 600 MHz, Tables S1, S2 (Supporting Information). The physical interpretation of Λ is somewhat more complex than a simple "fast exchange term" and deserves comment. In the fits of the dispersion profiles we have assumed that the intrinsic transverse relaxation rates due to the dipolar interactions that manifest within a methyl group are field independent. This is a very reasonable assumption, even in the context of unfolded proteins, as discussed below. However, it is not perfect. For example, focusing only on the dipolar terms, it is clear that $R_{2,int}$ rates will decrease (very slightly) with increasing field because spectral densities (see eq 2) decrease with increasing frequencies. This is not taken into account in our analysis and the discrepancy between dipolar contributions to $R_{2,int}$(800 MHz) and $R_{2,int}$(600 MHz) leads to decreased values of Λ and, in cases where there is no or little actual fast exchange, results in negative Λ values, as is observed for a number of residues (see Table S1, S2, Supporting Information). Thus, Λ must be considered as a lower bound for the exchange contributions. Finally, we have also fit our data to a model which assumes that $\Lambda = 0$ and find that very similar extracted dynamics parameters are obtained (Pearson correlation coefficient $R^2 = 0.91$ and rmsd in $\Delta(4J(0) + 3J(\omega_C))/4$ of 0.37 ns) although the quality of the fits is reduced.

As discussed above, the extracted relaxation parameters $4J^j(0) + 3J^j(\omega_C)$ are field dependent since $J(\omega_C)$ varies with field. In applications to folded proteins, however, $4J^j(0) + 3J^j(\omega_C) \approx 4J^j(0)$ and the field dependence is negligibly small. Indeed, even in cases where B corresponds to an unfolded state (as in the study here) the difference in $4J^B(0) + 3J^B(\omega_C)$ values at 500 and 800 MHz (^{1}H frequencies) is small, so that the inherent field dependence of the rates can be neglected. For example, in the case where $S^2_{axis} = 0.2$, $\tau_C = 1$ ns, $\tau_{axis} = 300$ ps, $\tau_{methyl} = 0$ the difference in $4J^B(0) + 3J^B(\omega_C)$ evaluated at $\nu_C = 125$ and 200 MHz is approximately 7% of $4J^B(0) + 3J^B(\omega_C)$ and this fractional difference decreases as τ_{methyl} increases. We have carried out a set of simulations to establish the significance of neglecting the field dependence of transverse relaxation rates in the analysis of our data. Using exchange parameters and intrinsic dynamics parameters in the computations that are similar to those obtained in fits of experimental data the errors in $\Delta(4J(0) + 3J(\omega_C))/4$ are small (<0.4 ns, well within typical experimental errors), with the extracted differences in intrinsic transverse rates (ground − excited) less than the actual differences.

Acknowledgment. We thank Dr. Sten Rettrup (Dept. of Chemistry, Univ. of Copenhagen) for helpful discussions and Professors Tony Mittermaier (Dept. of Chemistry, McGill University) and Voula Kanelis (Dept. of Chemistry, University of Toronto) for production of the Fyn SH3 domain and protein L samples. This work was supported by a grant from the Canadian Institutes of Health Research (CIHR) to L.E.K. D.F.H. acknowledges support in the form of a postdoctoral fellowship from the CIHR. L.E.K. holds a Canada Research Chair in Biochemistry.

Supporting Information Available: One figure showing that dynamics parameters can be separated from exchange rates, a second figure illustrating that errors from dynamic frequency shifts are small, a third figure showing *p*-values from fits as a function of extracted dynamics parameters, as well as tables of extracted exchange/dynamics parameters. The full author list of ref 18 is provided. This material is available free of charge via the Internet at http://pubs.acs.org.

JA903897E

(60) Kay, L. E.; Nicholson, L. K.; Delaglio, F.; Bax, A.; Torchia, D. A. *J. Magn. Reson.* **1992**, *97*, 359–375.